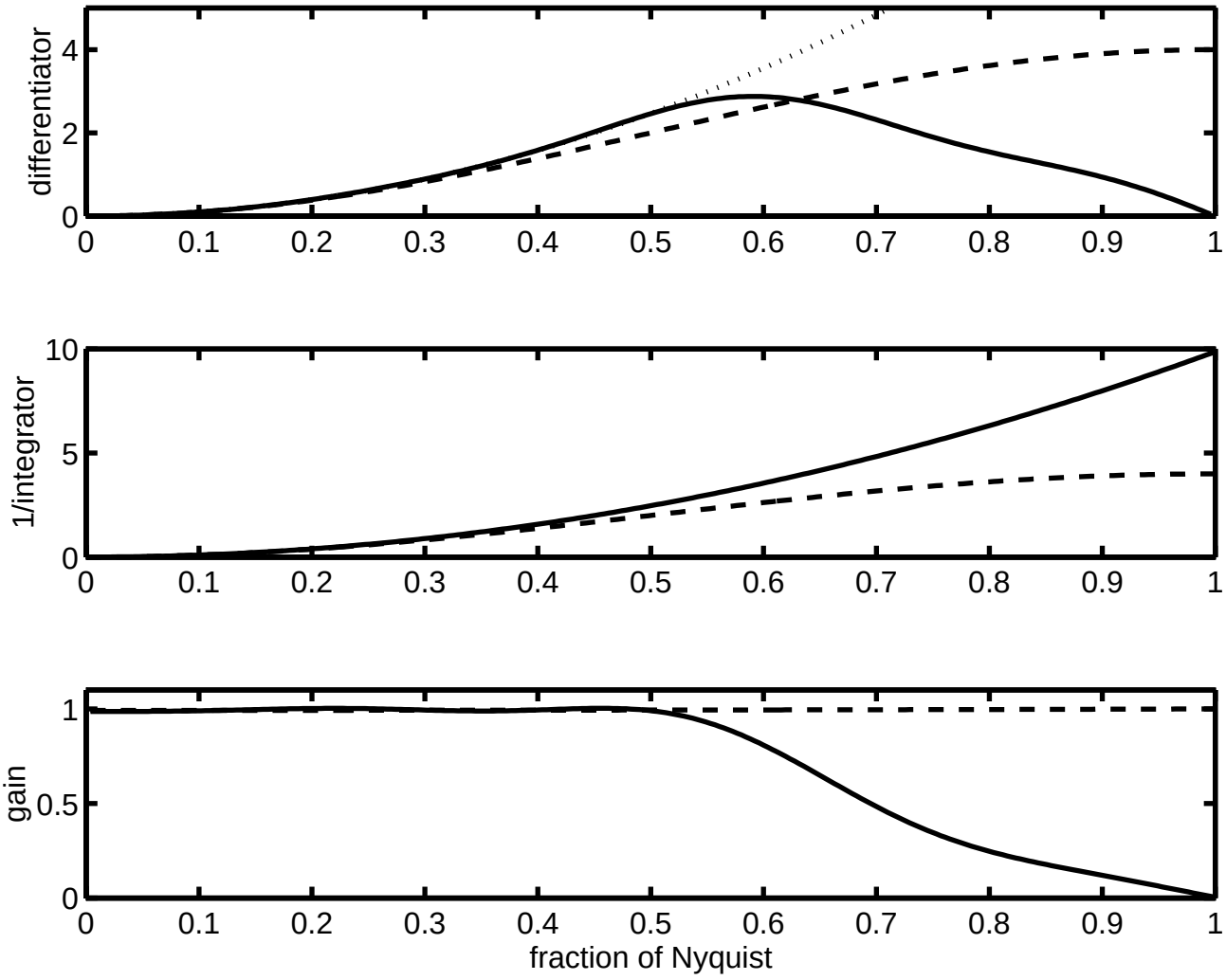

Figure 1. (top) Transfer functions of differential operators (dotted – ideal derivative, dashed – first difference, solid – Parks McClellan design see Figure 4). (middle) Inverse integral operator for first difference (dashed) and ideal derivative (solid). (bottom) Gain of combined differential operator followed by integral operator (dashed – first difference approach, solid – approach used in this paper). Note our approach has some signal loss at wavelengths shorter than 2 times the Nyquist wavelength.

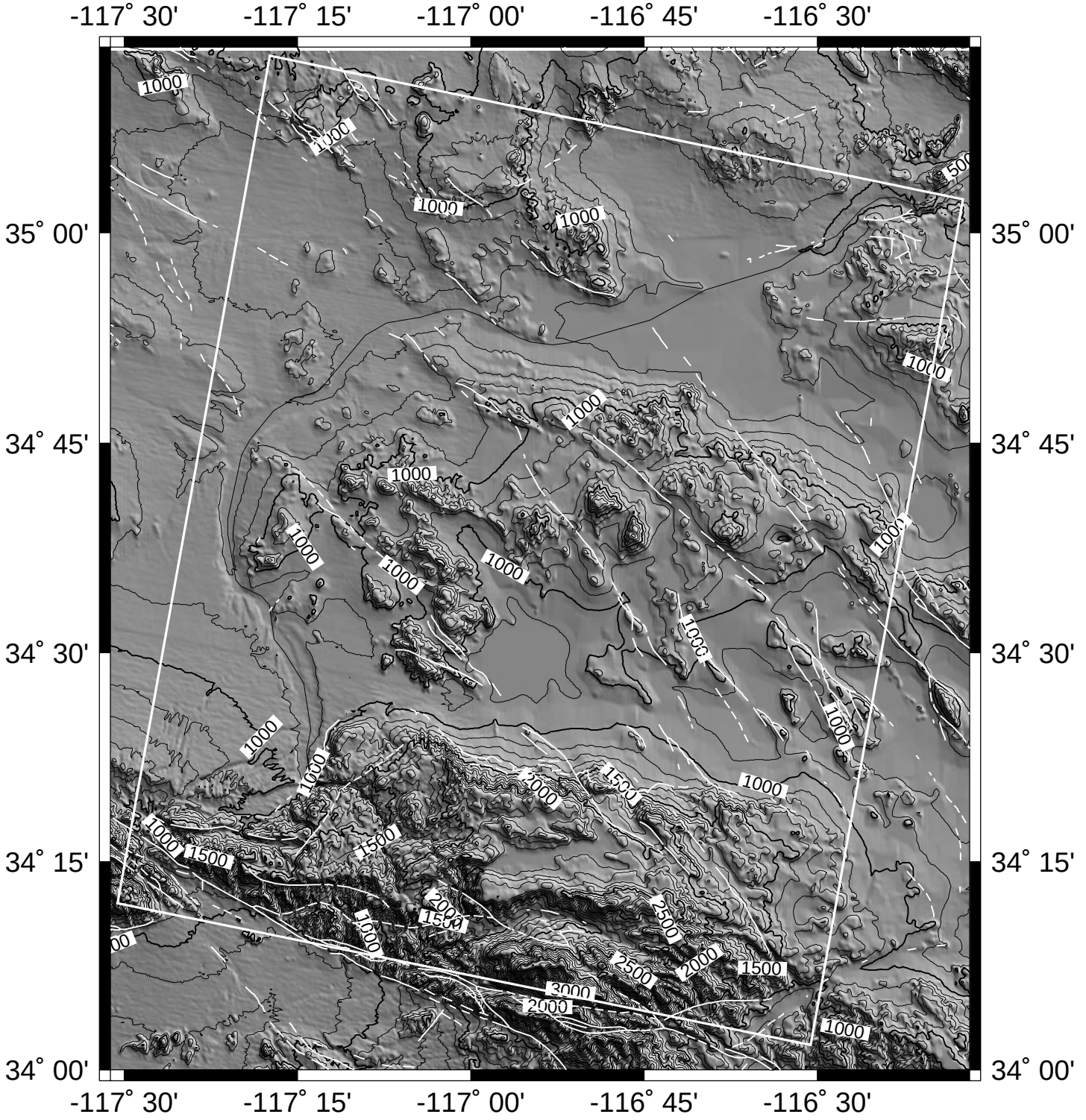

Figure 2. Shaded topography in Mojave Desert area (100 m contour interval). White box outlines area of ERS-1/2 SAR frame 2907 along a descending orbit. The Mojave River flows from southwest to northeast.

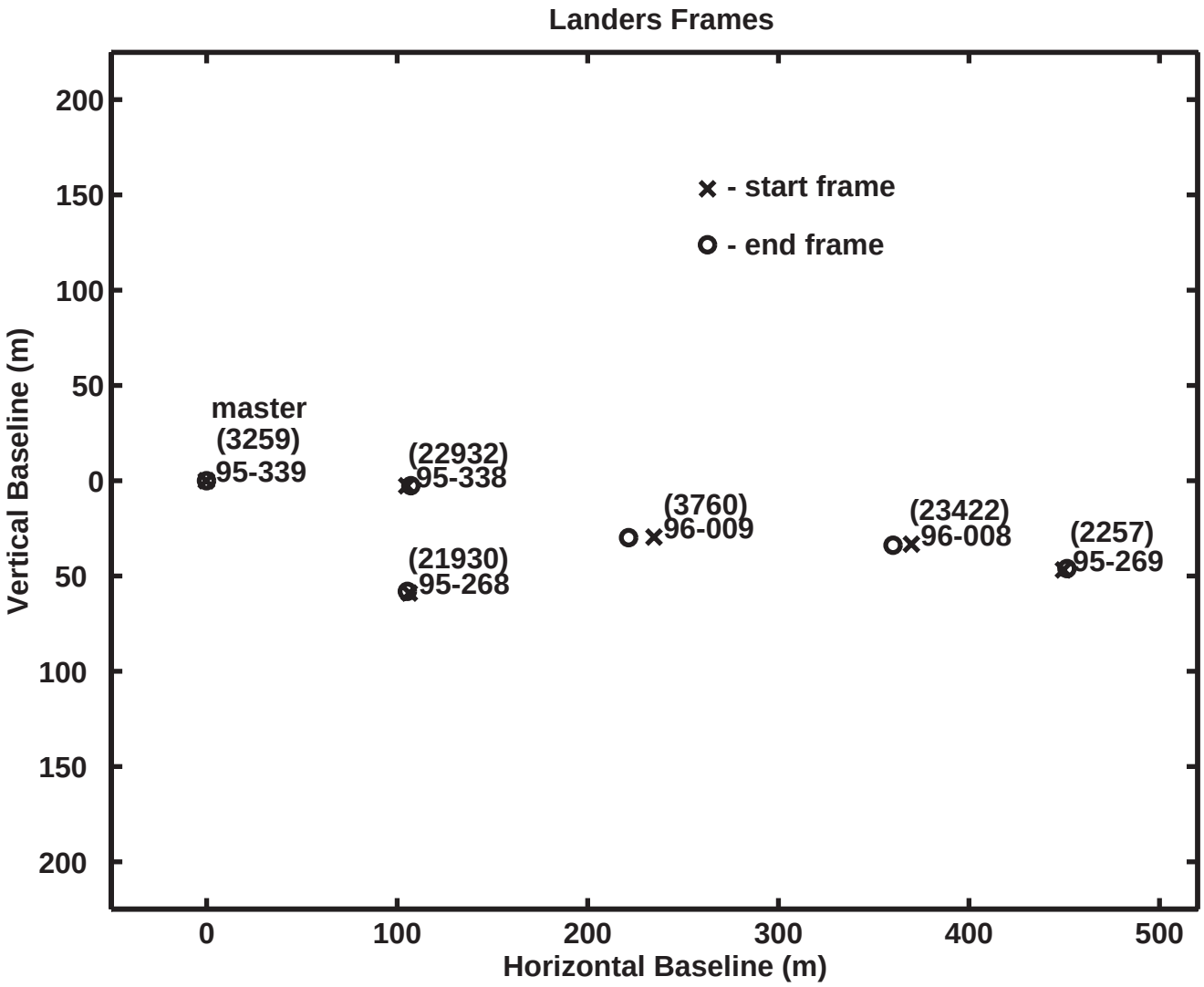

Figure 3. Positions of ERS orbits in relation to the master orbit (ERS-2 3259). Year and day-of-year are also provided. X shows satellite position at start of frame while O shows position at end of frame. Three pairs of SAR images are from the ERS-1/2 Tandem Mission and have 1-day time interval. For our analysis we used a suite of perpendicular baselines ranging from 18 m for 22923-21930 to 406.5 for 2257-3259.

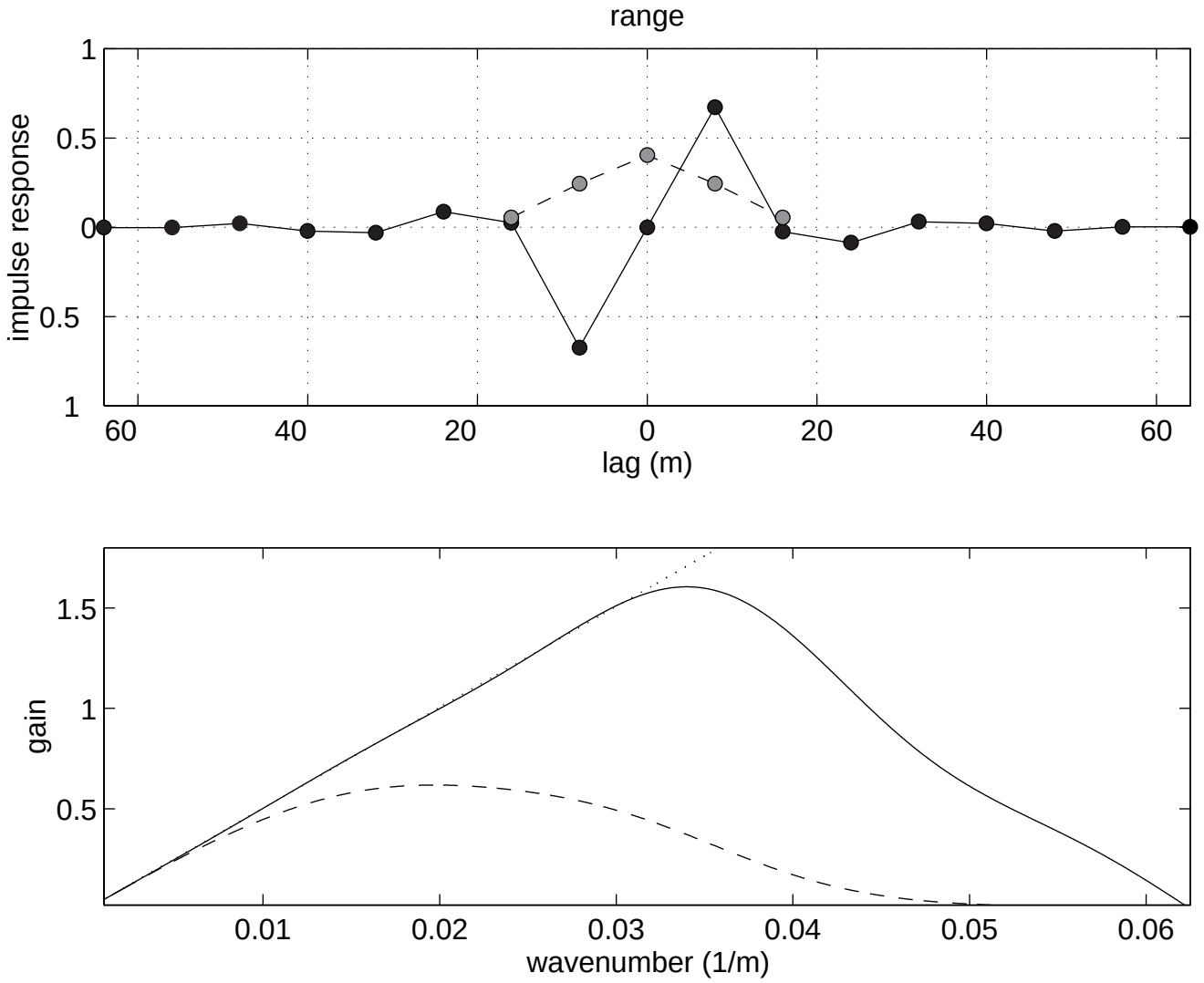

Figure 4. (upper) Low-pass Gaussian filter (grey dots) and derivative filter (black dots) applied to full resolution interferogram. (lower) Gain of ideal derivative filter (dotted line), 17-point convolution filter (solid curve) and Gaussian low-pass followed by 17-point derivative filter. The combined filter has nearly complete gain for wavelengths greater than 100 m.

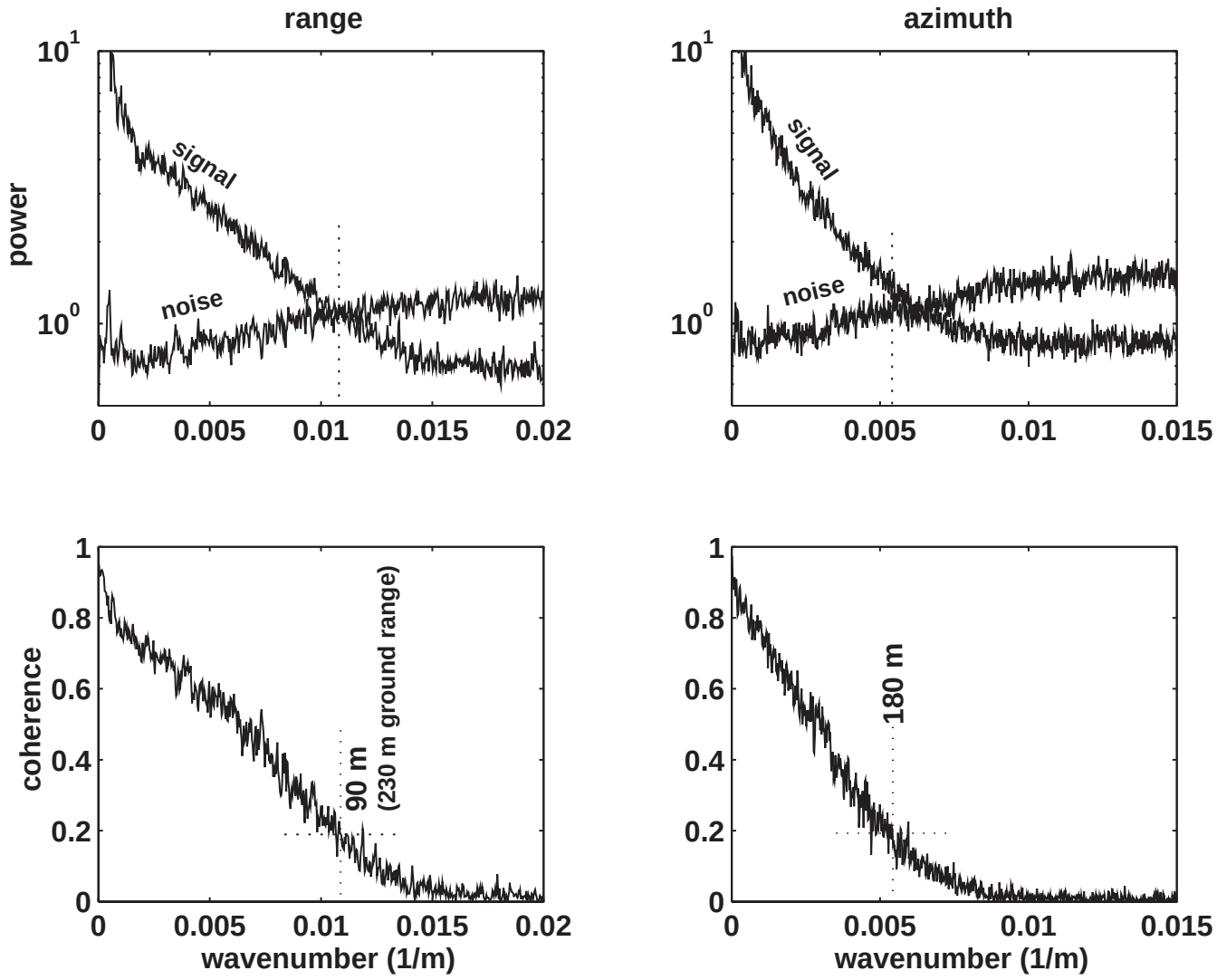

Figure 5. The correlation between phase gradients from tandem interferograms reveals the signal and noise as a function of wavenumber as well as the coherence versus wavenumber. The tandem interferograms (3rd and 4th row of Table 1) have similar baselines. For uncorrelated noise, a coherence of 0.2 marks a signal-to-noise ratio of 1 and provides a good estimate of the wavelength resolution of the data. Ground-range resolution is 230 m while azimuth resolution is 180 m. Stacking may provide better resolution so we design filters (Appendix B) to cut wavelength shorter than about 100 m from the full-resolution interferogram.

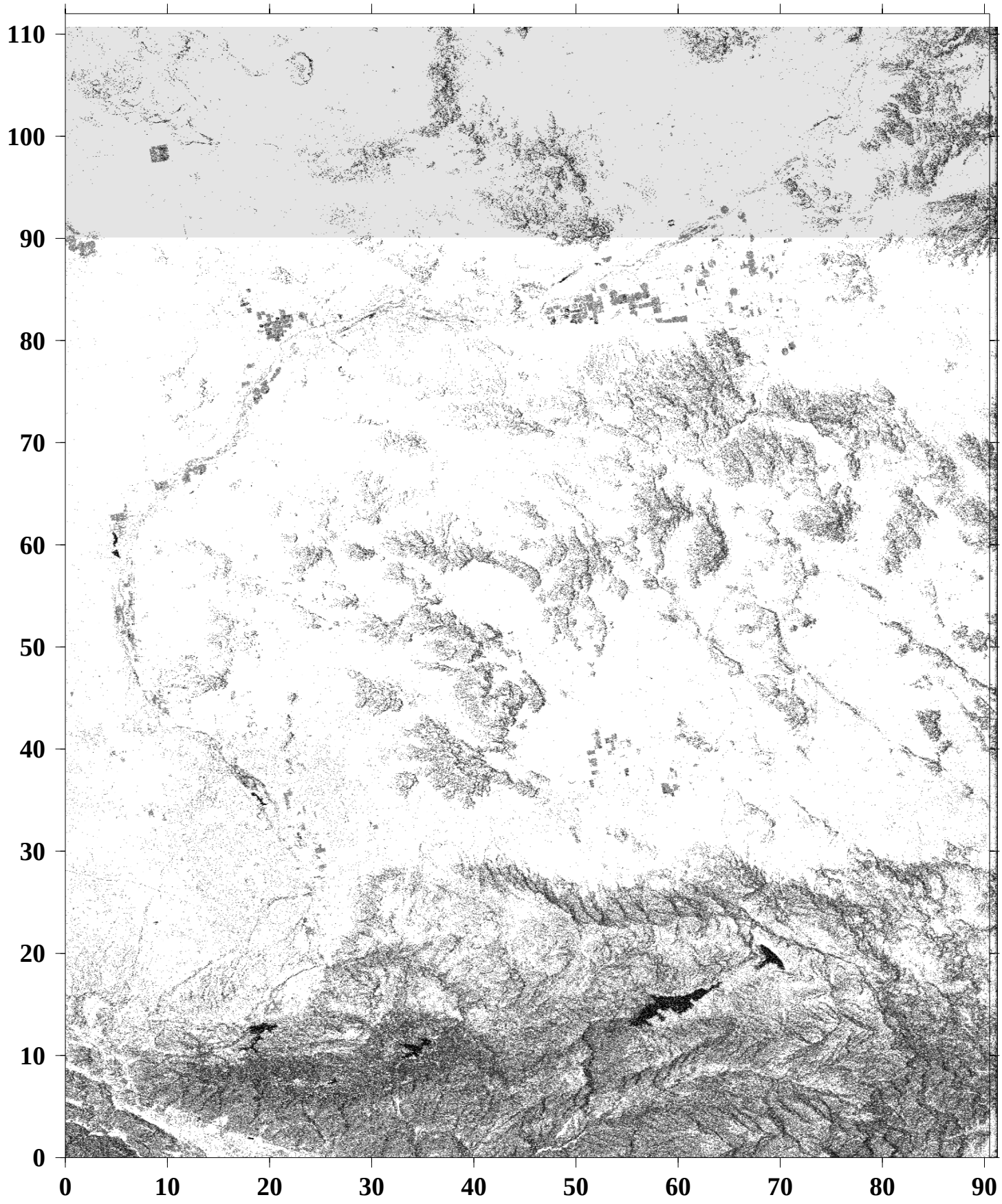

Figure 6. Cumulative baseline (range) shows the sum of the perpendicular baseline estimates that are available for stacking. Maximum baseline of 1050 m is white while zero baseline is black. The gray patch along the top reflects incomplete data from the 22932 ERS-1 frame. Other dark areas reflect decorrelation due to vegetation, standing water, and layover. Cumulative baseline is used to normalize the stack (equation 3) as well as to weight the iterative phase unwrapping for topographic recovery.

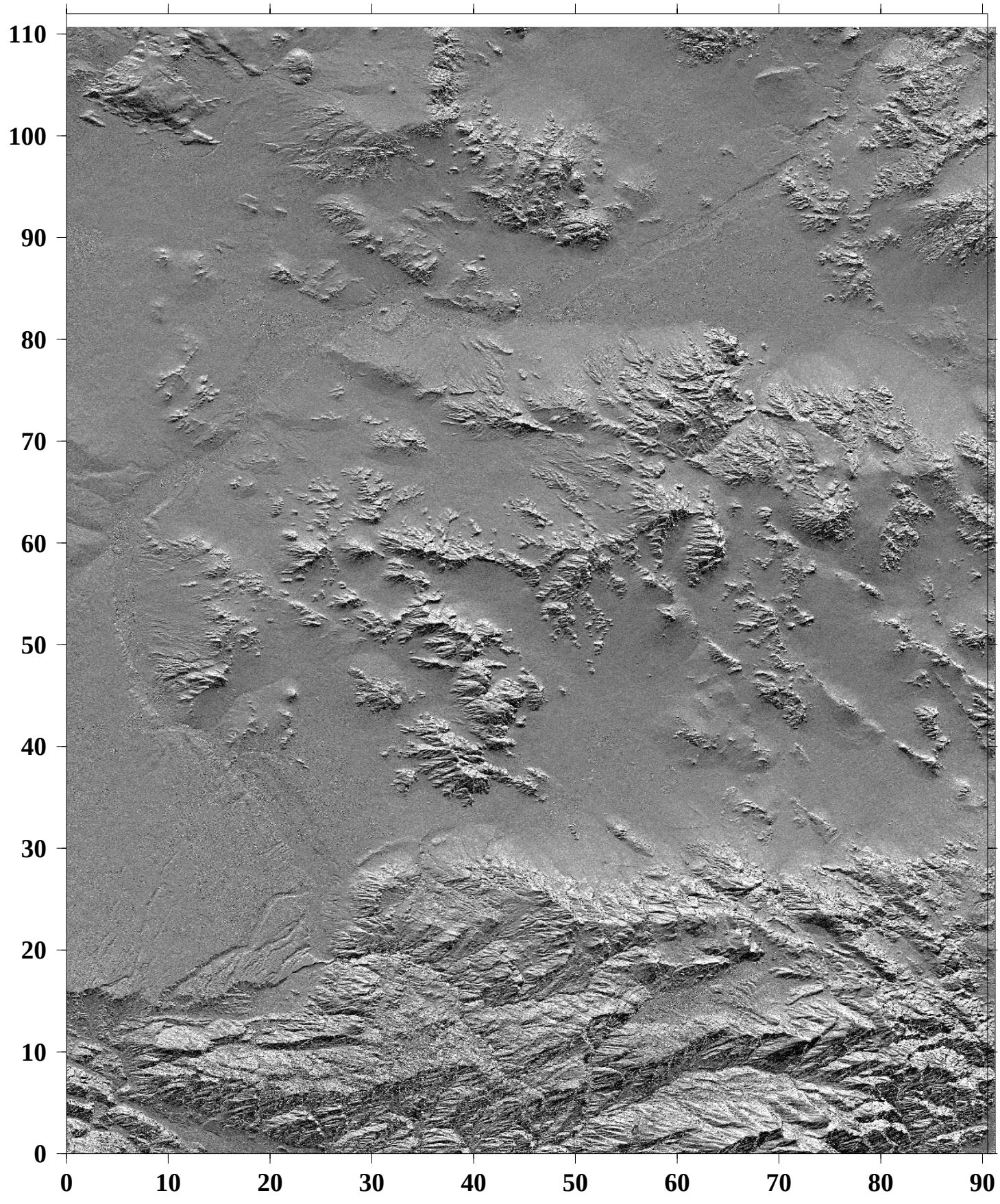

Figure 7. Stacked phase gradient in azimuth (black -.15 rad/pixel, white +.15 rad/pixel) appears as the topography illuminated from the north.

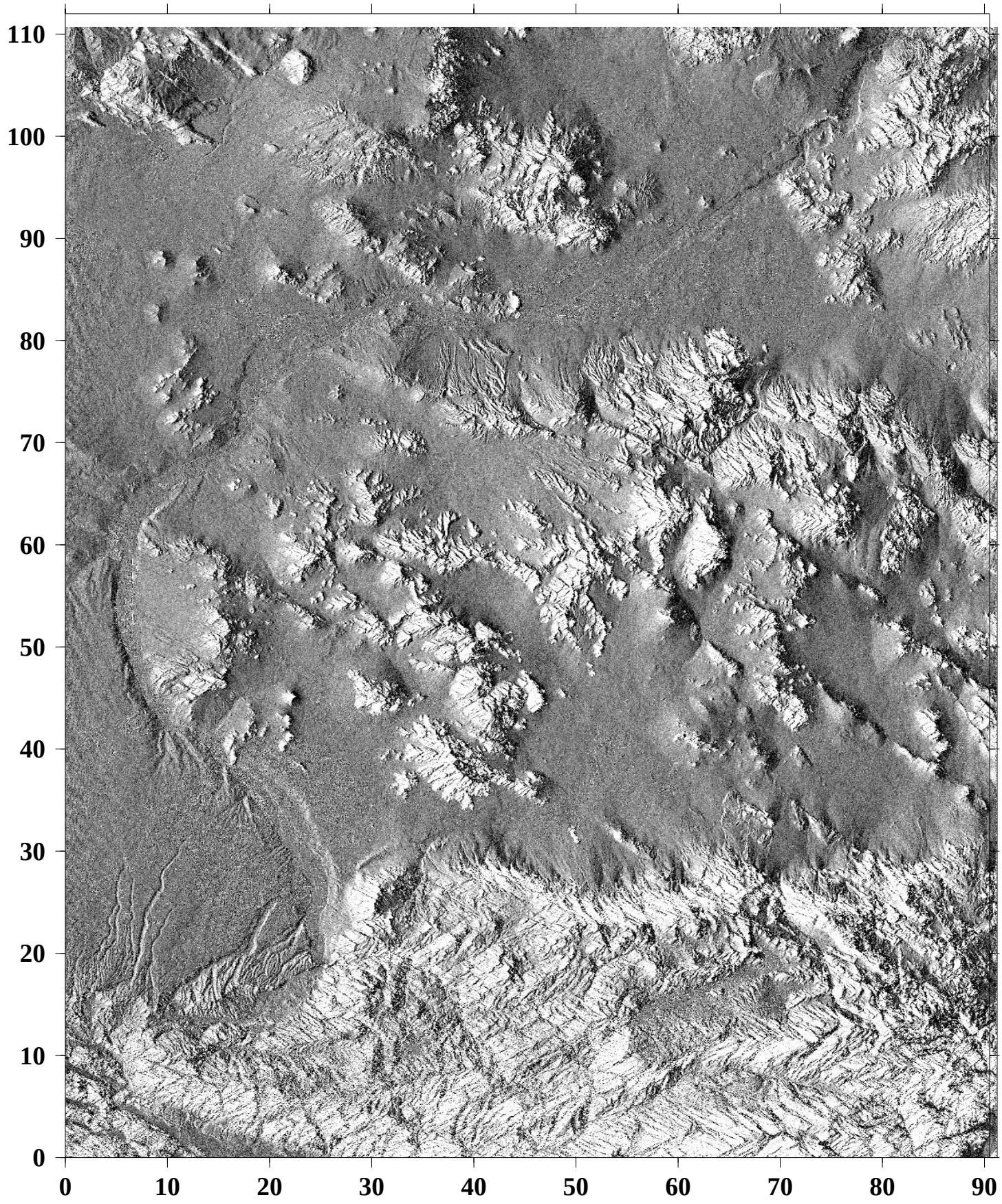

Figure 8. Stacked phase gradient in range appears as topography illuminated from the west. Note that in rugged areas such as the San Bernardino Mountians in the south, the slope distribution is asymmetric because the radar illuminates the eastern side of the mountains at a steep look angle of 20˚. This asymmetry, coupled with regions of complete layover, poses a significant problem in phase unwrapping.

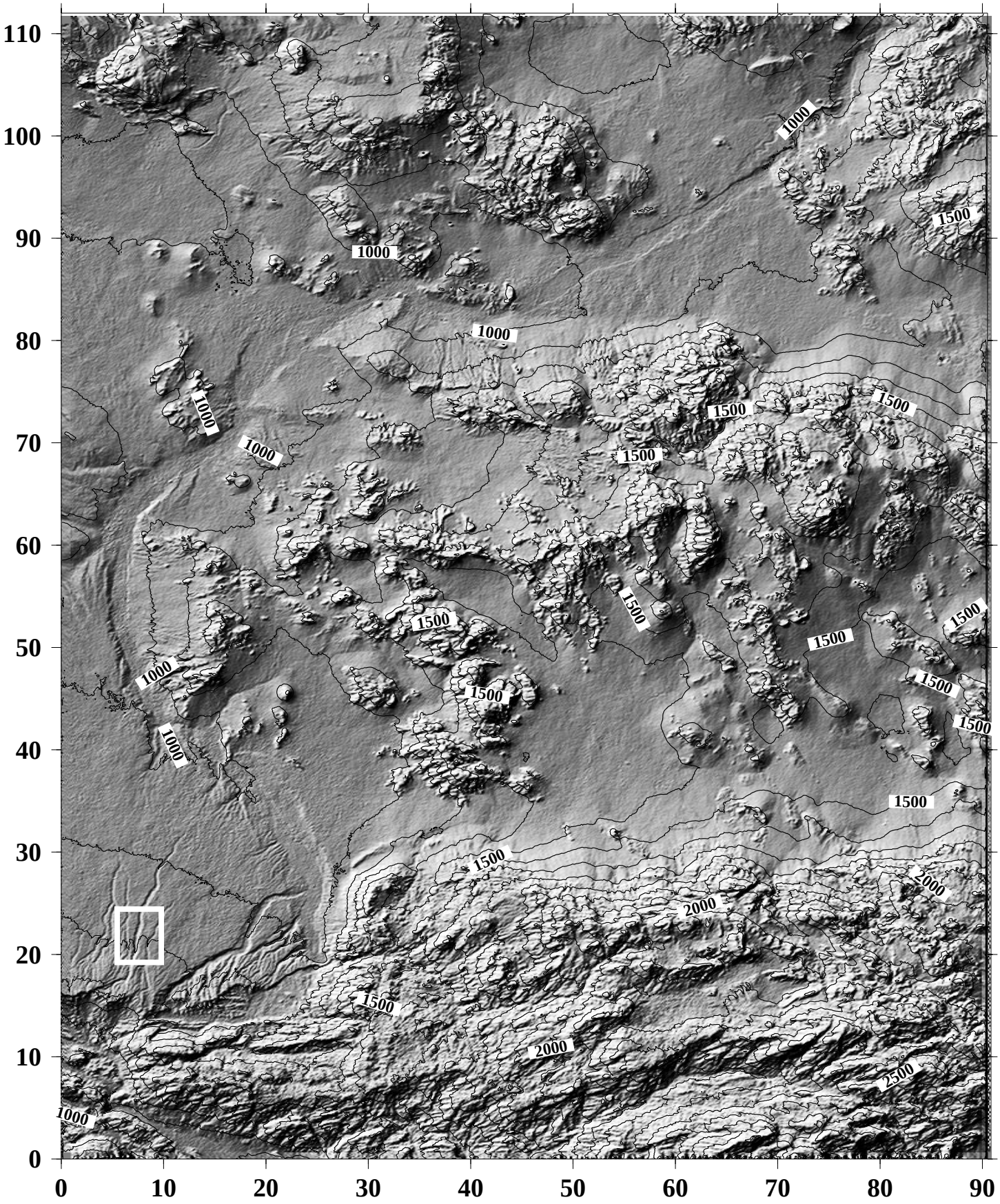

Figure 9. Unwrapped phase scaled into relief (A14) and contoured at 100 m intervals. At long wavelengths, the cumulative dropouts on the sides of the mountains facing the radar introduce long-wavelength errors in the unwrapped phase. On small scales, the relief estimates are quite detailed and accurate.

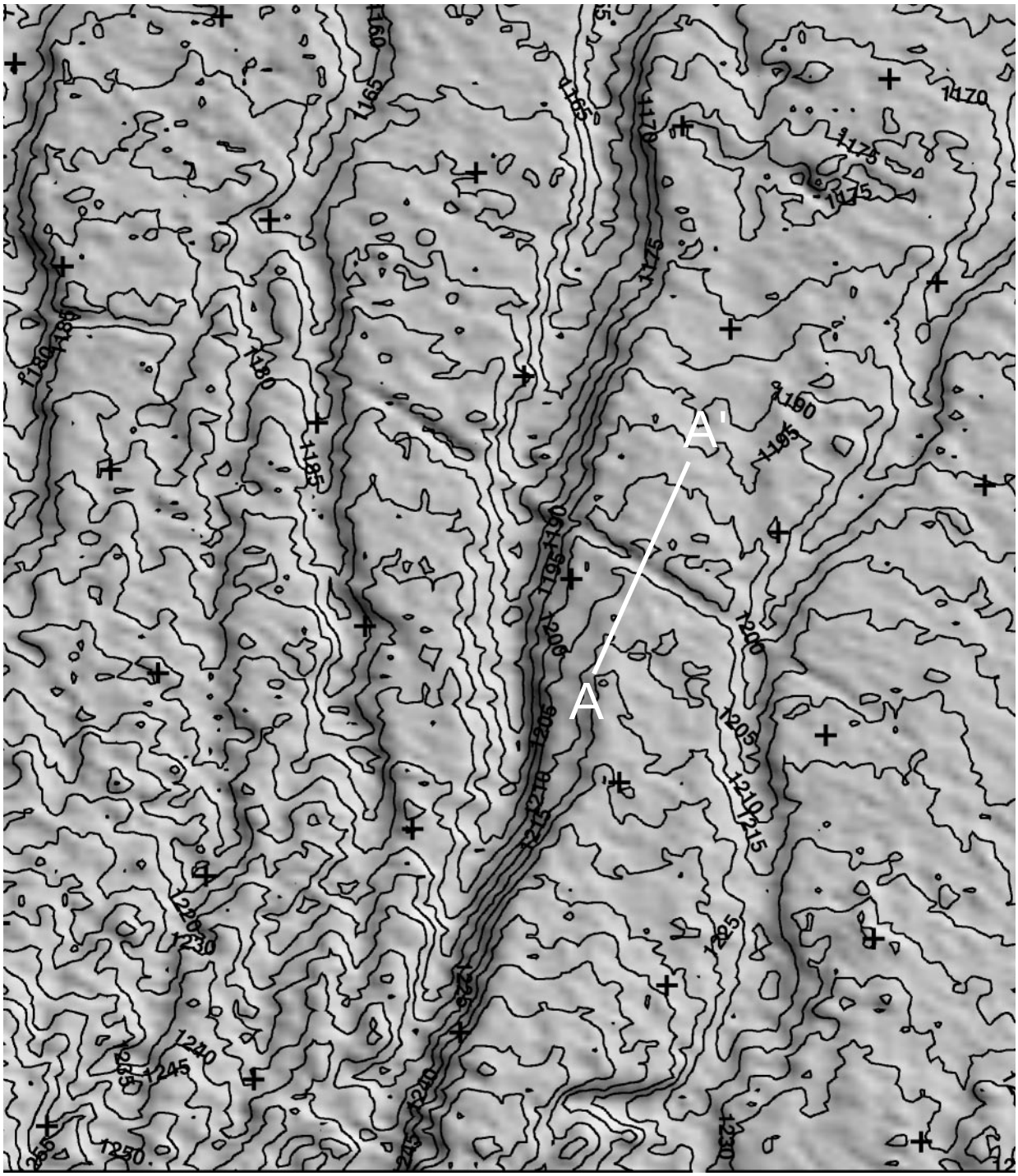

Figure 10. Topography of Oro Grande Wash (see red box on Figure 7) at a 5 meter contour interval. Tick marks are spaced at 1000 m intervals. White line marks a measured profile discussed in Appendix D. The overall depth of the Wash is 25 m. The Southern Pacific Railway trends northwest through the center of the image and appears as a 5-m deep trough in sloping surface surrounding the Wash. The track is elevated where it crosses the Wash.

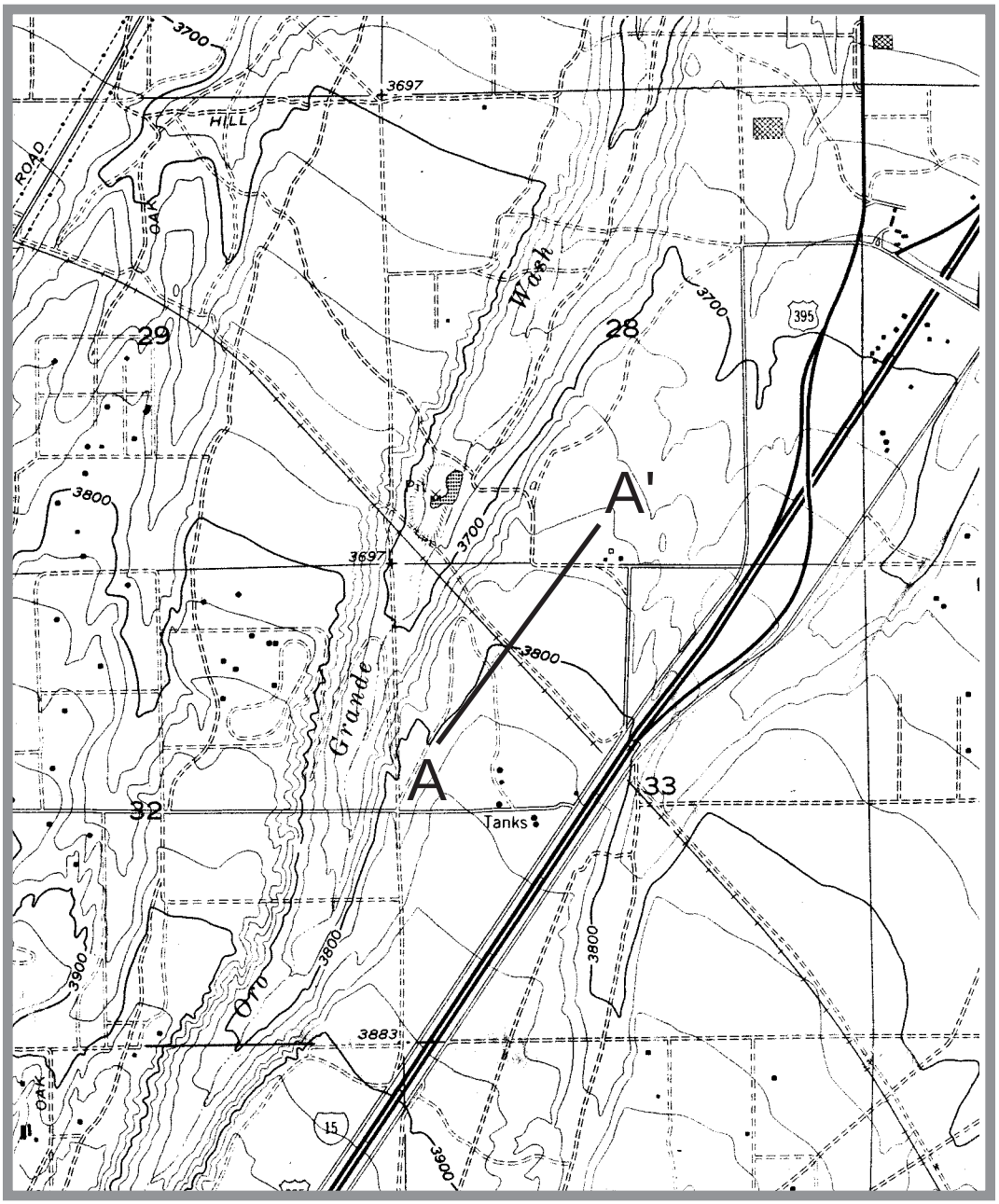

Figure 11. Contour map of Oro Grande Wash (20 foot contours) shows intersection with railway cut/fill. This should be compared with interferometric topographic recovery shown in Figure 8. Profile A - A' is 1000 m long

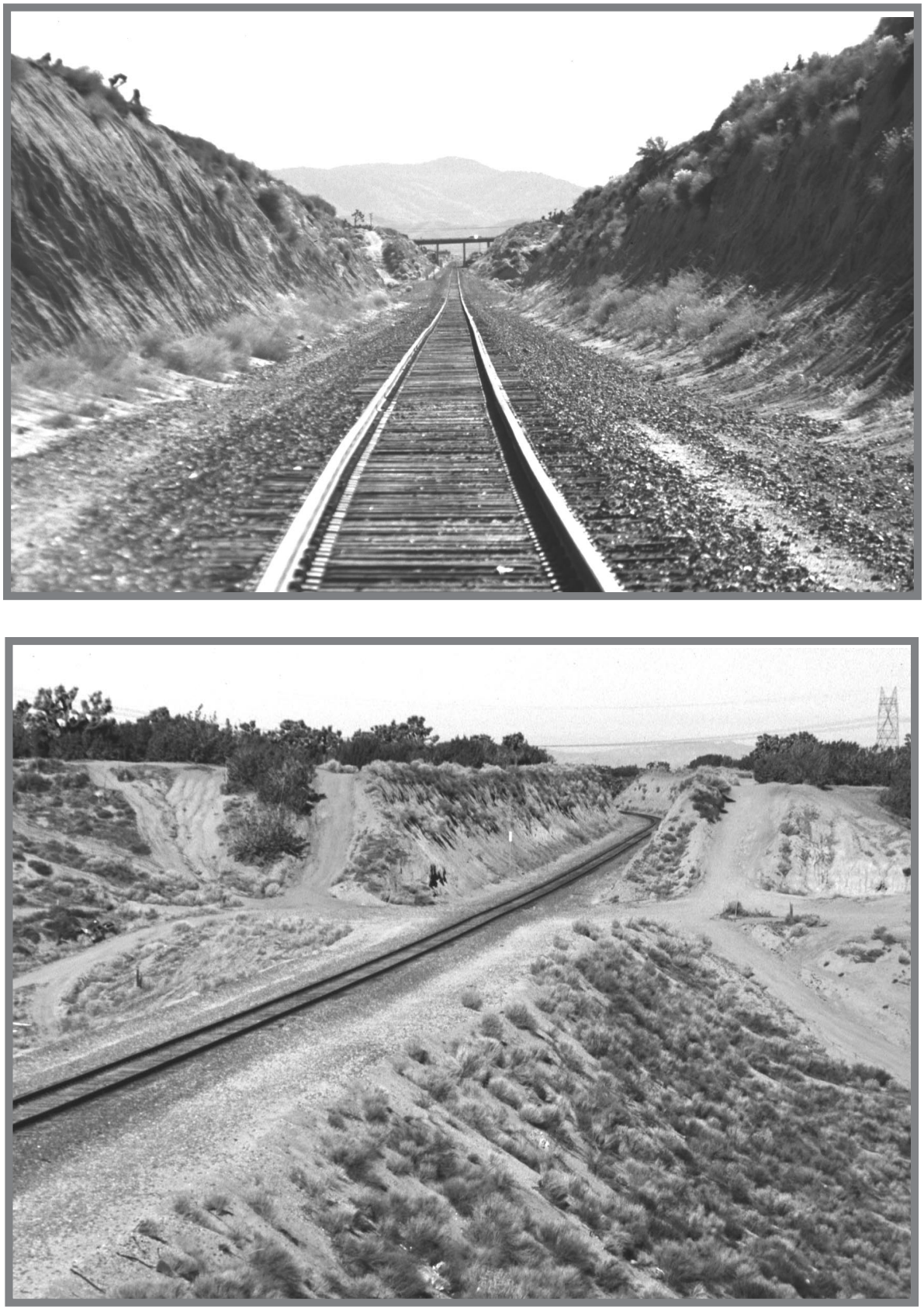

Figure 12. Photograph of cut and fill at Oro Grande Wash. (upper) looking southeast across wash with highway 15 in background. (lower) looking west at railway fill.

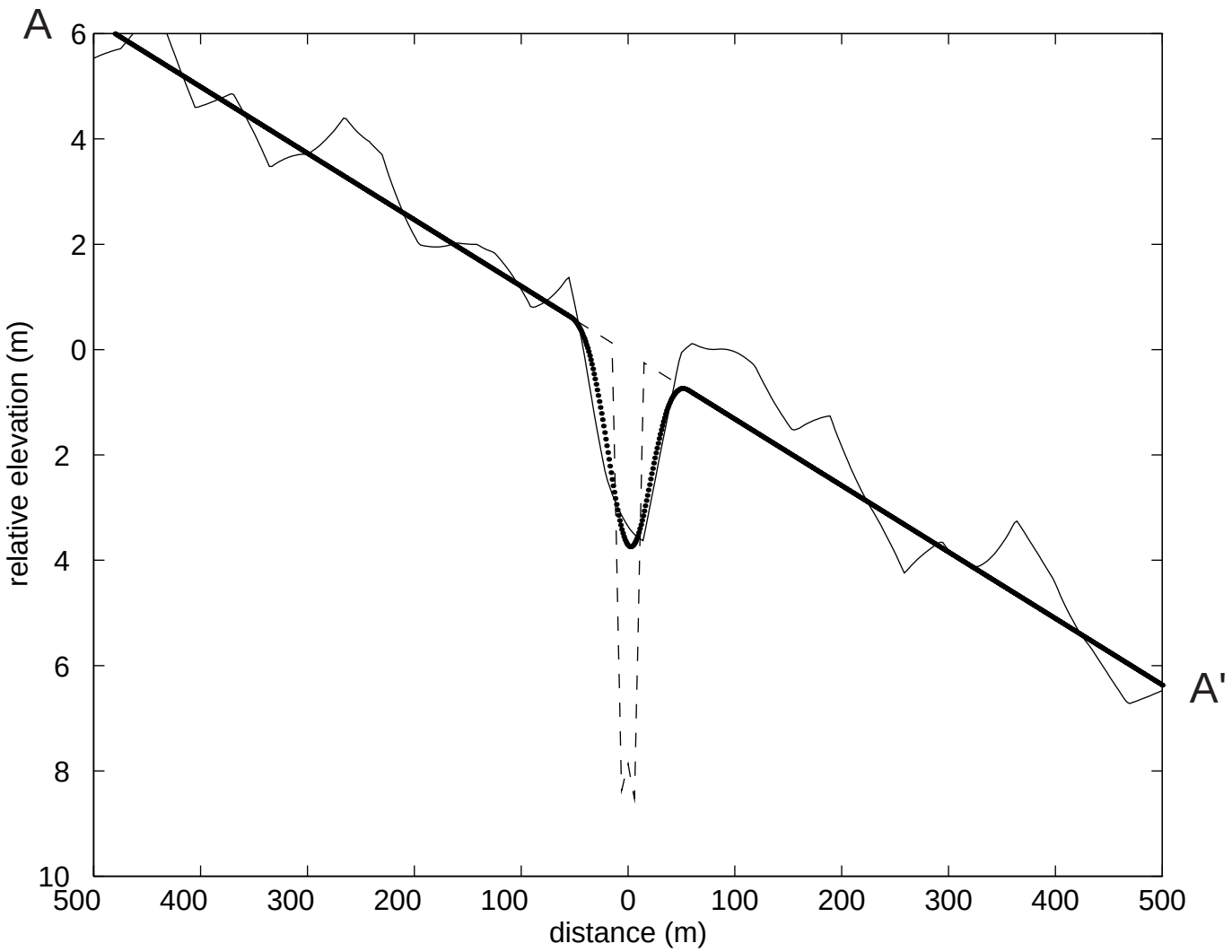

Figure 13. Profile A-A' across railway cut; solid curve from stacked interferogram, dashed curve is crude measurement of cut, dotted curve is measured topography convolved with Gaussian filter use to reduce noise in raw interferograms.

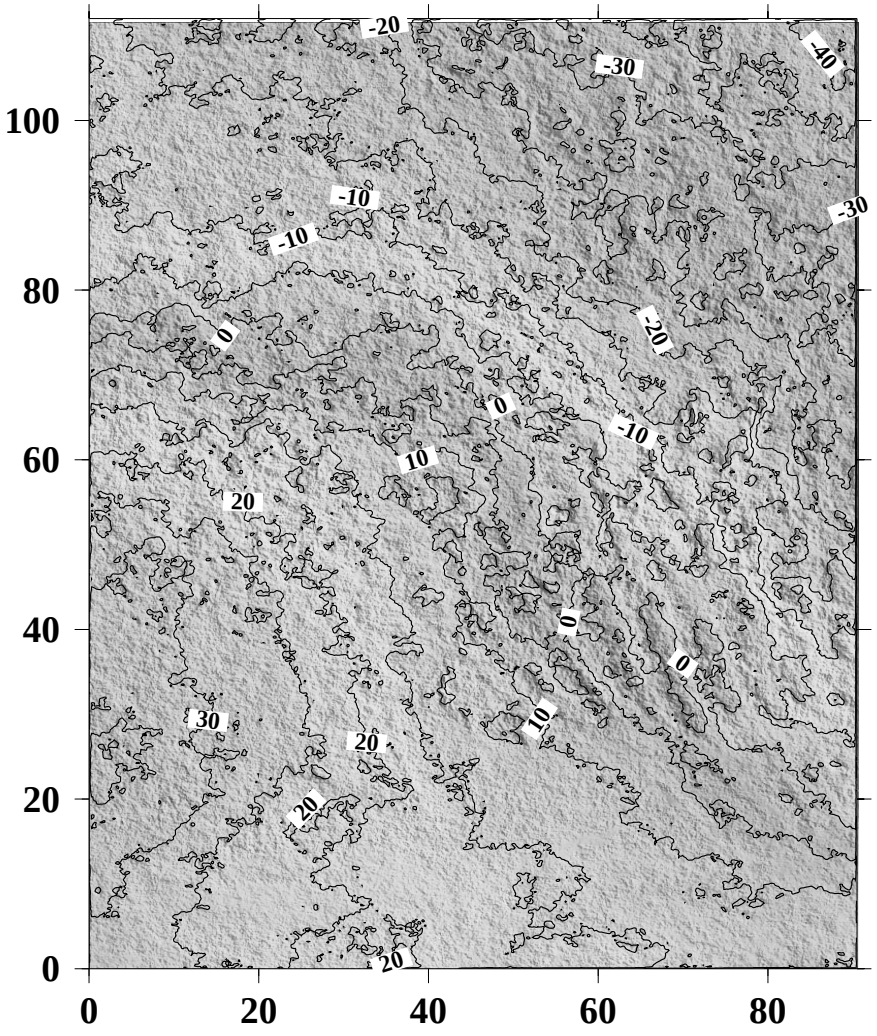

Figure 14. Unwrapped phase gradient difference for interferogram 2257-21930 having a perpendicular baseline of 327 m (5 mm contour interval). The stacked phase gradient was scaled to this baseline and removed from this interferogram. Unwrapping reveals a NE-SW trend that is related to orbit error and perhaps large scale atmospheric/ionospheric delays.

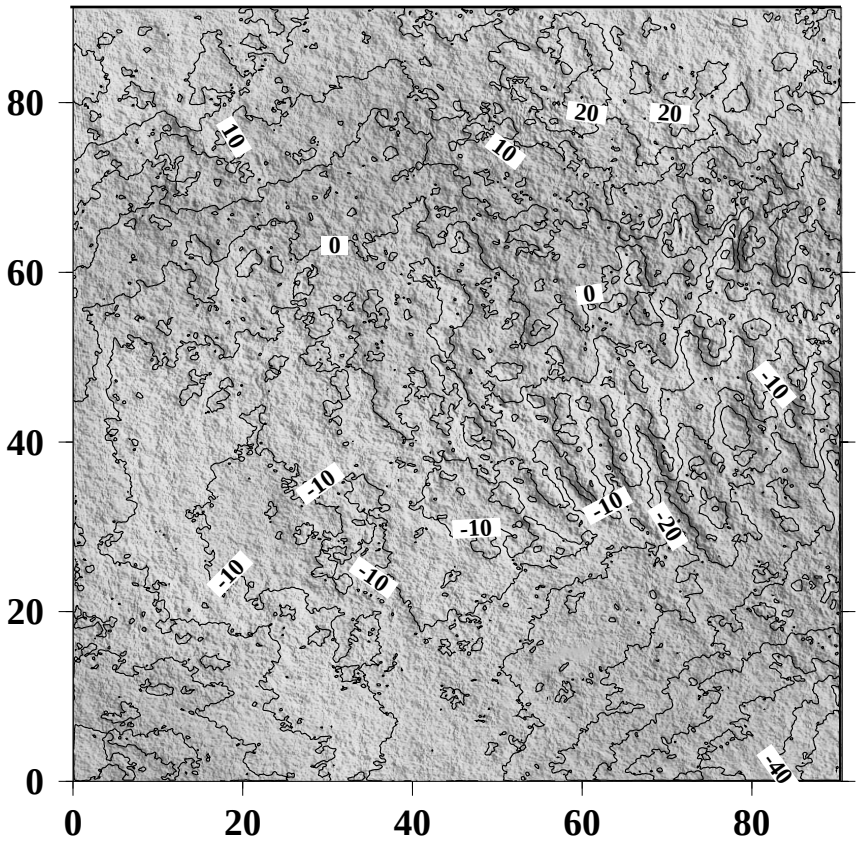

Figure 15. Unwrapped phase gradient difference for interferogram 22932-3259 having a perpendicular baseline of 97 m. We determined that 3259 was contaminated with atmospheric waves so a stack of three interferograms not containing 3259 was removed. The waves have characteristic amplitudes of 10-15 mm and wavelength of 5 km.

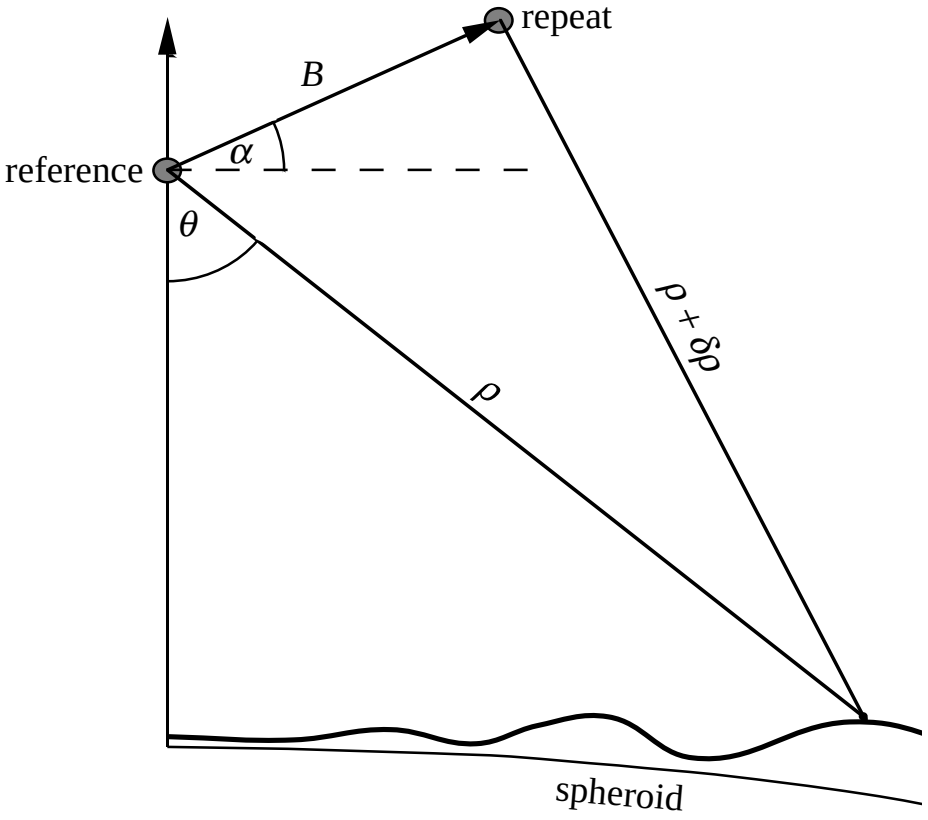

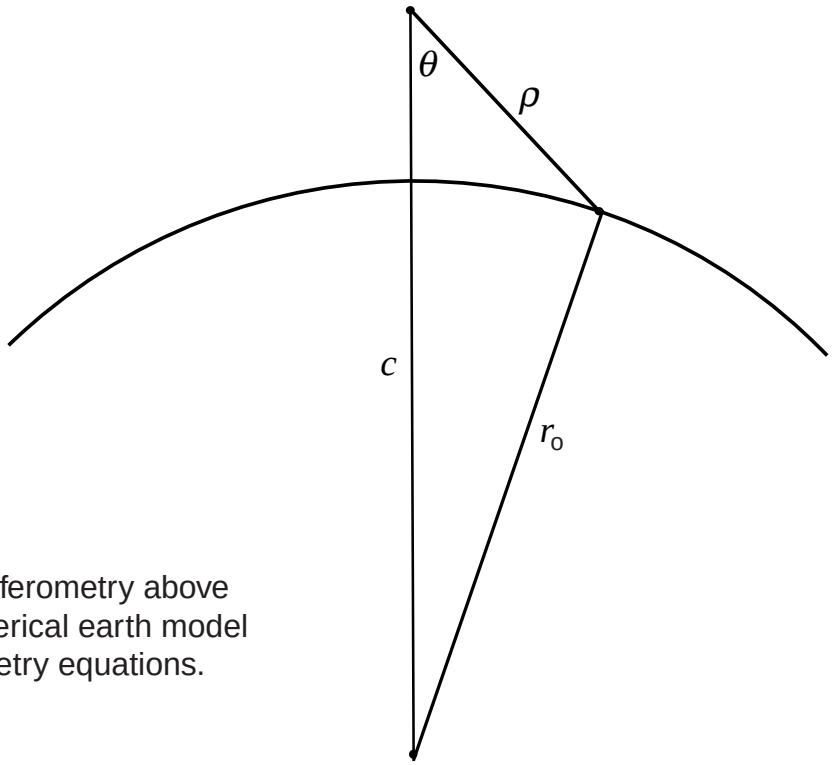

Figure A1. Geometry for interferometry above spherical earth model. A spherical earth model is used in all of the interferometry equations.